Association Efficiency of Three Ionic Forms of Oxytetracycline to Cationic and Anionic Oil-In-Water Nanoemulsions Analyzed by Diafiltration

SANDRA L. ORELLANA,[1] CESAR TORRES-GALLEGOS,[1] RODRIGO ARAYA-HERMOSILLA,[1] FELIPE OYARZUN-AMPUERO,[2] IGNACIO MORENO-VILLOSLADA[1]

[1]Instituto de Ciencias Químicas, Facultad de Ciencias, Universidad Austral de Chile, Valdivia, Chile
[2]Department of Sciences and Pharmaceutical Technology, University of Chile, Santiago, Chile

Received 27 May 2014; revised 7 October 2014; accepted 13 October 2014

Published online 29 December 2014 in Wiley Online Library (wileyonlinelibrary.com). DOI 10.1002/jps.24255

ABSTRACT: The association efficiency of oxytetracycline (OTC) to pharmaceutical available, ionic oil-in-water nanoemulsions is studied. Theoretical mathematical developments allowed us to differentiate by diafiltration (DF) between thermodynamically and kinetically controlled binding of the drug to the nanoemulsions, and relate these important magnitudes to the association efficiency. The nanoemulsions have been prepared by the solvent displacement technique in the presence of cationic and anionic surfactants. The resulting nanoemulsions were stable at 4°C and 25°C for 60 days, have a size of ∼200 nm, showing polydispersity indexes ranging between 0.11 and 0.23, and present zeta potentials ranging between −90 and +60 mV, depending on the charge of the surfactants used. The zeta potential of the nanoemulsions influenced the interaction with OTC, having three ionic forms at different pH, namely, cationic, zwitterionic, and anionic. DF proved to be a powerful tool for the quantification of the drug association efficiency, achieving values up to 84%. Furthermore, this technique allowed obtaining different values of the drug fractions reversibly bound (11%–57%) and irreversibly bound (10%–40%) to the nanoemulsions depending on the surfactants used and pH. These findings may be useful for the development of new drug delivery systems, and as routine assays in academia and pharmaceutical industries. © 2014 Wiley Periodicals, Inc. and the American Pharmacists Association J Pharm Sci 104:1141–1152, 2015

Keywords: oil-in-water nanoemulsions; surfactants; encapsulation; oxytetracycline; diafiltration; mathematical model; drug interactions; thermodynamics; kinetics

INTRODUCTION

Micro- and nanoemulsions have found applications in many fields since a long time ago. Oil-in-water nanoemulsions ($NE_{O/W}$) involve oil droplets dispersed in aqueous medium. Reported sizes of nanoemulsified oil droplets are among 20 and 500 nm.[1–3] In order to disperse and stabilize the nanodroplets, different types of surfactants can be used. Among them, ionic surfactants are widely studied.[4–6] Ionic $NE_{O/W}$ present high stability due to the electrostatic repulsions between the charged surfaces of the functionalized droplets, so that they can persist over months. Although nanoemulsions are only kinetically stable systems, long-term physical stability of nanoemulsions (with no apparent flocculation or coalescence) is referred to as *approaching thermodynamic stability*, as is the case of ionic $NE_{O/W}$.[7] Ionic surfactants play an important role in the physicochemical characteristics of nanoemulsions, such as stability, size, shape, and interfacial tension.[8] The arrangement of the electric charge at the oil droplet surface is generally modeled as an electric double layer, according to the Stern model, a combination of the Helmholtz and Gouy-Chapman models.[9,10] Ions in the inner layer are strongly bound to the droplet surface, whereas ions in the outer layer, of opposite charge, are less firmly associated. The balance between the van der Waals attraction and the electric double layer repulsion determines the stability of $NE_{O/W}$.[11] An approximated calculation of the electric potential at this second layer is given by the measurement of electrokinetic potential (zeta potential), corresponding to the potential on the surface of the shear between the moving particle and the bulk when the system is submitted to an external electric field.

Applications of $NE_{O/W}$ in medicine aims at solubilizing and carrying lipophilic bioactive compounds for their use in cancer treatment, ocular therapies, vaccination, and administration of anti-inflammatory drugs.[12] They also find a wide application field in health care staff and cosmetics because the large surface area of the emulsion system allows rapid penetration in tissues.[13,14] The association concept is pivotal in pharmaceutical sciences. The binding of a low-molecular-weight species (LMWS), such as drugs, to large species (namely, high-molecular-weight species, molecular assemblies, solids, etc.), may be thermodynamically or kinetically controlled. In kinetically controlled systems, such as molecules confined in capsules, solids, or polymeric matrices, the release of the active molecules is normally controlled by diffusion or erosion. On the contrary, in thermodynamically controlled systems, such as liposomes, nanoemulsions, and vesicles,[15,16] the release of the molecules of interest is determined by the equilibrium constants. Thus, fast kinetics of molecular exchange between different phases occurs, and the corresponding distribution of the molecules responds to the free energy of the system.

The interaction of LMWS with the nanodroplets in ionic $NE_{O/W}$ should be considered thermodynamically controlled, as no physical barrier is established at the interface. In this

Correspondence to: Ignacio Moreno-Villoslada (Telephone: +56-632293520; Fax: +56-632293520; E-mail: imorenovilloslada@uach.cl)

Journal of Pharmaceutical Sciences, Vol. 104, 1141–1152 (2015)

sense, misinterpretation of the physicochemical behavior of the LMWS may occur under the scope of the encapsulation concept, as molecules considered encapsulated are in fact undergoing fast exchange with non-encapsulated ones. However, the partition coefficient of hydrophobic LMWS between the aqueous phase and the hydrophobic core tends to zero in most cases, and the confinement of such molecules in the nanodroplets is referred as encapsulation in the literature, thus acting as kinetically controlled.[17,18] On the contrary, hydrophilic LMWS are difficult to encapsulate in the hydrophobic core. Despite this, hydrophilic LMWS may also interact with the nanodroplets in ionic $NE_{O/W}$ because of the electrostatic interactions with the droplet charged surfaces. Under the scope of the Stern model, the counterions should arrange both in the double electric layer and in the bulk. The electric double layer is deduced by the counterion condensation theory applied to spheres developed by G.S. Manning. This theory is an extension of the Debye–Hückel theory, and is based on long-range electrostatic interactions. This theory deduces that counterions condense forming a layer of hydrated counterions around charged spheres of charge density over a certain threshold, whose value depends on the size of the sphere.[19,20] The condensed counterions are territorially bound, that is, the binding is not site-specific concerning any functional group of the charged sphere. This theory was first developed in order to analyze counterion binding to linear polyelectrolytes,[21–23] and was further expanded to objects with different geometries.[19,20] However, for organic counterions, deviations from expected results have been reported, ascribed to the occurrence of site-specific short-range interactions.[24–28] Indeed, the hydrocarbon nature of organic counterions and their structure may produce hydrophobic interactions related with the amphiphilia of the LMWS, and secondary short-range interactions such as short-range electrostatic interactions, hydrogen bonding, and aromatic–aromatic interactions that change the interaction patterns, producing site-specific binding, higher binding constants, specific molecular geometries and architectures, and even binding of like-charged molecules.[24–26,28–31] In particular, aromatic–aromatic interactions may easily produce ion pairs of high hydrophobia that may be stabilized in a hydrophobic environment,[32,33] affecting the partition coefficient. For systems thermodynamically controlled, the equilibrium established between the interacting molecules is sensitive to the environmental conditions.[30,34]

In the case of kinetically controlled nanosystems, it is usually presented centrifugation as a method to calculate drug encapsulation efficiency and drug release from the nanovehicles.[35–37] By this method, the nanocarriers are concentrated at the top or at the bottom of the centrifugation tubes, allowing by direct or indirect mass balance calculating the referred parameters. However, for thermodynamically controlled systems such as $NE_{O/W}$, ultracentrifugation produces stress in the formulations, destabilizes the nanovehicles, and affects the partition equilibrium and/or diffusion of drugs, leading to misinterpretation of the results.[38–40] Alternative methods to evaluate drug release from $NE_{O/W}$ are dialysis and ultrafiltration, from which a single value of drug partition between the nanocarrier and the bulk is obtained in each experiment.[38,41,42]

The diafiltration (DF) technique is based on the separation of different chemical species according to their molecular mass, and has been used to prepare and purify nanoobjects such as nanocapsules or virus.[43–45] Complex mixtures are filtered through a membrane, which has pores that discriminate between species according to their molecular size. In addition, as a separation technique, DF has emerged as an effective technique to study interactions between LMWS and several macromolecular species including soluble polymers,[25–28,30–34,46–50] polymeric nanoparticles,[51,52] antibodies,[53] and food matrices,[54] among others. The membrane pore size may be chosen so that only the passage of free LMWS is allowed.[48] An advantage of the constant volume DF technique is that it allows differentiating kinetically controlled systems, if the release kinetics are much lower than the filtration kinetics, from thermodynamically controlled systems, if the kinetics of equilibrium are much faster than the filtration kinetics. For the latter case, a distribution constant can be calculated from the DF profiles referring the ratio of molecules free in the bulk versus those reversibly bound to the system. Thus, the fraction of molecules whose binding is kinetically controlled can be obtained, as well as the fraction of molecules thermodynamically bound. DF constitutes a simple, cheap, and continuous method, which can be regarded as the succession of infinite dialysis or ultrafiltration steps of infinitely low volume filtration. Based on this, the use of DF is presented here as an attractive alternative for determining the binding nature and efficiency of LMWS to $NE_{O/W}$, that find potential application in the pharmaceutical industry to characterize pharmaceutical formulations and achieve quality control.

Tetracyclines are broad spectrum antibacterials that exhibit activity against a large range of Gram-positive and Gram-negative bacteria. Oxytetracycline (OTC) is an antibiotic belonging to the tetracycline family used in animal and human health. Its approved uses in humans include the treatment of respiratory, genitourinary, and cutaneous infections. Among available formulations in the market, we can find pills, drops, and ointments. Tetracyclines inhibit bacterial protein synthesis by binding the 30s ribosomal subunit, specifically the aminoacyl site A. Its mechanism of action involves preventing the binding of aminoacyl–tRNA to the acceptor site ribosomal mRNA–ribosome complex, and consequently, the inhibition of the addition of new amino acids to the growing peptide chain.[55] Their indiscriminate use in food animal production could lead to important sanitary risks for humans such as bacterial resistance, allergies, ossification and dentition problems, and carcinogenic effects. Different investigations have shown that after passing through waste water treatment, biologically active compounds are released directly into the environment.[56] In the case of OTC, being a broad spectrum antibiotic, the selection and development of a variety of pathogenic-resistant bacteria is one of the greatest concerns.[57,58] Importantly, spread of resistance may occur by direct contact or indirectly, through food, water, and animal waste application to farm fields.[59] Nanotechnological formulations may offer advantages for the administration and delivery of drugs that may be useful to prevent and overcome problems derived from overuse.[60] Polymeric nanoparticles, liposomes, solid lipid nanoparticles, nanoemulsions, and dendrimers have been widely investigated as antimicrobial drug delivery systems.[61] However, the inclusion of OTC in nanovehicles may be difficult because of its high affinity towards water.

In this paper, we will highlight the use of DF to evaluate the association efficiency (AE) of hydrophilic drugs to nanovehicles, and we will report, for the first time, a DF study on the interaction of a hydrophilic organic model drug, OTC, with cationic and anionic $NE_{O/W}$. By the use of DF, we will give insights about the nature of the interaction and the physicochemical behavior

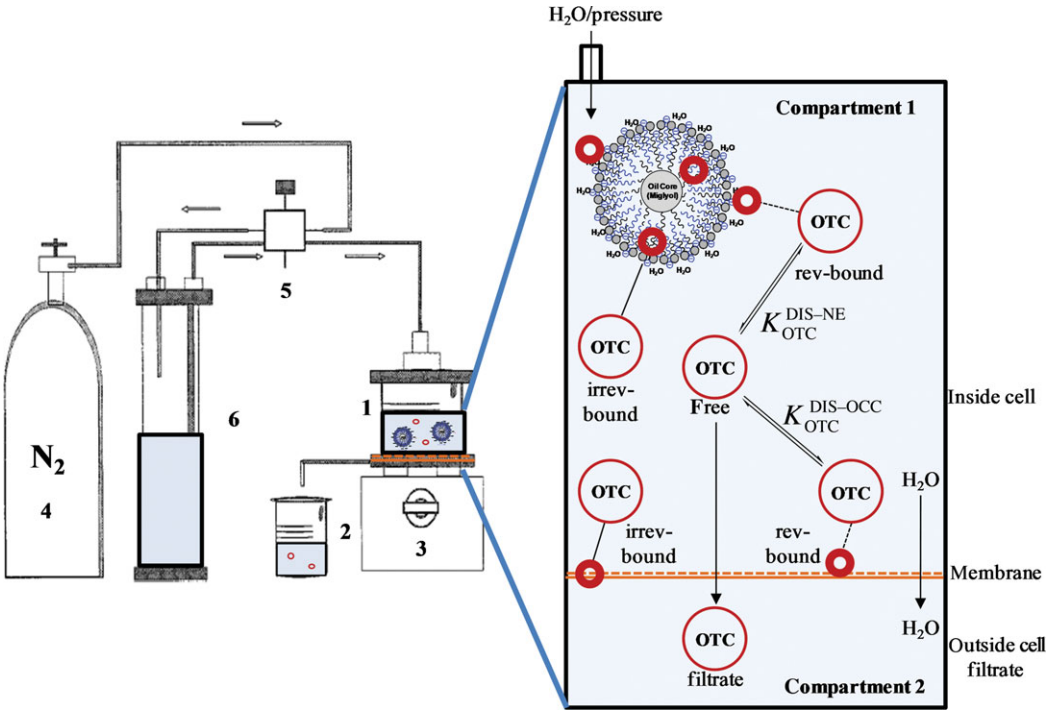

Figure 1. DF equipment showing the DF cell with membrane (1), filtrate (2), magnetic stirrer (3), pressure source (4), selector (5), and reservoir (6), and schematic molecular dynamics inside the cell solution.

of the nanosystems, and search the corresponding association efficiencies, distinguishing molecules in three states: free in the bulk, kinetically bound, and thermodynamically bound to the $NE_{O/W}$. The prepared $NE_{O/W}$ comprises components approved for pharmaceutical uses, in order to guarantee the potential of the formulations to be used in the pharmaceutical industry.

THEORY

The association of drugs to macromolecular formulations in solution may be taken in a wide sense, comprising thermodynamically bound and kinetically bound molecules.[31,48,50,62] The respective molar fractions of molecules bound by each mechanism can be denoted by TB_f and KB_f, respectively. Thus, the drug AE, denoting the total fraction of drug bound independently of the mechanism of binding, is given by

$$AE = TB_f + KB_f \tag{1}$$

The DF system consists of a filtration cell, a DF membrane, a reservoir, a selector, and a pressure source (see Fig. 1). The DF cell has been modeled as a two compartment system, both compartments separated by the DF membrane. By creating a continuous flux of liquid through the cell solution from the reservoir, the volume in the cell (V^{cell}) is kept constant. The filtration factor (F) is defined as the volume ratio of the filtrate ($V^{filtrate}$) versus V^{cell}. The distribution of molecules in every instant is schematically depicted in Figure 1 for the system OTC/$NE_{O/W}$. The main magnitudes associated to the different states of OTC in the system in the DF analysis are the concentration of OTC free in the cell solution (c_{OTC}^{free}), the concentration of OTC irreversibly bound to the $NE_{O/W}$, ($c_{OTC}^{irrev-bound-NE}$), and the concentration of OTC reversibly bound to the $NE_{O/W}$, ($c_{OTC}^{rev-bound-NE}$); as the drug may also interact with any of the cell components, (mainly the membrane due to its large effective surface area), the concentrations of OTC irreversibly and reversibly bound to the cell components are also considered ($c_{OTC}^{irrev-bound-OCC}$ and $c_{OTC}^{rev-bound-OCC}$, respectively). By irreversibly bound we consider molecules bound in processes that may be reversible with apparent distribution constants, considering the ratio between free and bound molecules, that tend to zero at the conditions of the experiment, or confined molecules showing release kinetics slower than the DF kinetics. Finally, OTC, as a hydrophilic LMWS, is able to traverse the DF membrane and may be found in the first layer of the filtrate, at the boundary with the membrane in compartment 2, with an instantaneous concentration given $c_{OTC}^{filtrate}$by .

Important concepts lead us to mathematical important equations:

1. A mass balance of OTC inside the cell may be expressed as

$$c_{OTC}^{cell} = c_{OTC}^{irrev-bound-NE} + c_{OTC}^{irrev-bound-OCC} + c_{OTC}^{rev-bound-NE} + c_{OTC}^{rev-bound-occ} + c_{OTC}^{free} \tag{2}$$

2. By definition, only OTC in its free state inside the cell is able to traverse the membrane, so that, in every instant

$$c_{OTC}^{free} = c_{OTC}^{filtrate} \tag{3}$$

3. On the other hand, during filtration, a balance can be established between the mass change in the cell and in the filtrate, so that

$$V^{\text{cell}}\mathrm{d}c_{\text{OTC}}^{\text{cell}} = -c_{\text{OTC}}^{\text{filtrate}}\mathrm{d}V^{\text{filtrate}} \tag{4}$$

or, in other

$$\mathrm{d}c_{\text{OTC}}^{\text{cell}} = -c_{\text{OTC}}^{\text{filtrate}}\mathrm{d}F \tag{5}$$

4. Finally, the behavior of the system is assumed to be linear, so that the fraction of OTC reversibly bound to the $NE_{O/W}$ or any of the other cell components is dominated by distribution constants defined as

$$K_{\text{OTC}}^{\text{DIS-NE}} = \frac{c_{\text{OTC}}^{\text{free}}}{c_{\text{OTC}}^{\text{rev-bound-NE}}} \tag{6}$$

$$K_{\text{OTC}}^{\text{DIS-OCC}} = \frac{c_{\text{OTC}}^{\text{free}}}{c_{\text{OTC}}^{\text{rev-bound-OCC}}} \tag{7}$$

Substituting Eqs. (6) and (7) in Eq. (2) and rearranging, we obtain that

$$c_{\text{OTC}}^{\text{cell}} = c_{\text{OTC}}^{\text{irrev-bound-NE}} + c_{\text{OTC}}^{\text{irrev-bound-OCC}} + c_{\text{OTC}}^{\text{free}}\left[\frac{1}{K_{\text{OTC}}^{\text{DIS-NE}}} + \frac{1}{K_{\text{OTC}}^{\text{DIS-OCC}}} + 1\right] \tag{8}$$

Combination of Eq. (3) with Eq. (8) followed by derivation, substitution of the resulting equation in Eq. (5), and integration leads to the following important expression, related with the evolution of OTC during filtration,

$$c_{\text{OTC}}^{\text{filtrate}} = c_{\text{OTC}}^{\text{filtrate-init}}e^{-jF} \tag{9}$$

where *init* is referred to initial conditions, that is, $F = 0$, and

$$j = \frac{1}{\frac{1}{K_{\text{OTC}}^{\text{DIS-NE}}} + \frac{1}{K_{\text{OTC}}^{\text{DIS-OCC}}} + 1} \tag{10}$$

On the other hand, Eq. (9) can be combined with Eq. (5), and after integration, another important expression, related with the evolution of OTC during filtration, is obtained:

$$c_{\text{OTC}}^{\text{cell}} = c_{\text{OTC}}^{\text{cell-init}}\left[u + ve^{-jF}\right] \tag{11}$$

where

$$v = \frac{c_{\text{OTC}}^{\text{filtrate-init}}}{c_{\text{OTC}}^{\text{cell-init}}j} \tag{12}$$

and

$$u = 1 - v \tag{13}$$

or, in other words

$$c_{\text{OTC}}^{\text{cell}} = c_{\text{OTC}}^{\text{cell-init}}\left[1 - \underbrace{\frac{C_{\text{OTC}}^{\text{filtrate-init}}}{C_{\text{OTC}}^{\text{cell-init}}j}}_{u = \text{OTC irreversibly bound fraction at } F = 0} + \underbrace{\frac{C_{\text{OTC}}^{\text{filtrate-init}}}{C_{\text{OTC}}^{\text{cell-init}}j}}_{v = \text{OTC reversibly bound fraction at } F = 0}e^{-jF}\right] \tag{14}$$

Note that Eqs. (9) and (11) indicate an exponential decay of the concentration of OTC both in the filtrate and in the cell as DF proceeds. The parameters u and v represent the fraction of OTC irreversibly and reversibly bound to any of the cell components including the $NE_{O/W}$ at $F = 0$, before diafiltering, respectively. The parameter j is related to the strength of the interaction corresponding to the reversibly bound fraction, thus thermodynamically controlled, as it contains the distribution constants. The same treatment can be performed in the absence of the nanoemulsion as control in blank experiments, and the parameters u^{m}, v^{m}, and k^{m}, corresponding to u, v, and j, respectively, are obtained by applying the same mathematical treatment, where the terms corresponding to the $NE_{O/W}$ are omitted. Thus, the actual value of the distribution constant concerning the drug and the $NE_{O/W}$ can be obtained from Eq. (10) as

$$K_{\text{OTC}}^{\text{DIS-NE}} = \frac{jk^{\text{m}}}{k^{\text{m}} - j} \tag{15}$$

because

$$K_{\text{OTC}}^{\text{DIS-OCC}} = \frac{k^{\text{m}}}{1 - k^{\text{m}}} \tag{16}$$

Derivation of Eq. (11) and substitution in Eq. (5), and combination of the resulting equation with Eqs. (3), (6), (7), (15), and (16), allow calculating the amounts of drug reversibly bound to any of the cell components in every instant during filtration. Thus,

$$c_{\text{OTC}}^{\text{rev-bound-NE}} = c_{\text{OTC}}^{\text{cell-init}}\frac{k^{\text{m}} - j}{k^{\text{m}}}ve^{-jF} \tag{17}$$

and

$$c_{\text{OTC}}^{\text{rev-bound-OCC}} = c_{\text{OTC}}^{\text{cell-init}}\frac{1 - k^{\text{m}}}{k^{\text{m}}}jve^{-jF} \tag{18}$$

In addition, the amounts of drug irreversibly bound can directly be calculated by the expressions

$$c_{\text{OTC}}^{\text{irrew-bound-NE}} = c_{\text{OTC}}^{\text{cell-init}}(u - u^{\text{m}}) \tag{19}$$

because

$$c_{\text{OTC}}^{\text{irrev-bound-OCC}} = c_{\text{OTC}}^{\text{cell-init}}u^{\text{m}} \tag{20}$$

On the contrary, as the filtrate is collected in discrete filtration fractions of relative volume ΔF, the experimental value of $c_{\text{OTC}}^{\text{filtrate-init}}$ obtained is an average ($< c_{\text{OTC}}^{\text{filtrate-init}} >$) value, so that

DOI 10.1002/jps.24255

a correction factor must be added to the calculation of v.[31,50] Thus

$$v = -\frac{< c_{\mathrm{OTC}}^{\mathrm{filtrate-init}} > \Delta F}{c_{\mathrm{OTC}}^{\mathrm{cell-init}} \left[1 - \exp\left(j\,\Delta F\right)\right]} \tag{21}$$

The DF analyses allow, then, obtaining information about the distribution of the drug in the cell at any instant. For the original formulation, the fraction of OTC reversibly bound to the $NE_{O/W}$, is given after combining Eqs. (6) and (12) by the formulae

$$\mathrm{TB_f} = \frac{c_{\mathrm{OTC}}^{\mathrm{rev-bound-NE-init}}}{c_{\mathrm{OTC}}^{\mathrm{cell-init}}} = \frac{j v}{K_{\mathrm{OTC}}^{\mathrm{DISS-NE}}} = \frac{v\left(k^{\mathrm{m}} - j\right)}{k^{\mathrm{m}}} \tag{22}$$

and the fraction of OTC irreversibly bound to the $NE_{O/W}$, is given from Eq. (19) by

$$\mathrm{KB_f} = \frac{c_{\mathrm{OTC}}^{\mathrm{irrev-bound-NE-init}}}{c_{\mathrm{OTC}}^{\mathrm{cell-init}}} = u - u^{\mathrm{m}} \tag{23}$$

Thus, substituting Eqs. (22) and (23) in Eq. (1)

$$\mathrm{AE} = \frac{v\left(k^{\mathrm{m}} - j\right)}{k^{\mathrm{m}}} + u - u^{\mathrm{m}} \tag{24}$$

MATERIALS AND METHODS

Reagents

The mixture of surfactants EPIKURON™ 145V (EPIK) was donated by Cargill: Minnetonka, Minnesota, United States. Hexadecyl trimethyl ammonium bromide (CTAB), benzalkonium chloride (BKC), and SDS were used as cosurfactants and purchased from Sigma–Aldrich®. Oxytetracycline dihydrate (OTC) was used as received from Sigma–Aldrich®. The structure of OTC as a function of the pH is shown in Figure 2, together with the structure of the cosurfactants. The mineral oil Migyol 812 was donated by Laboratorio Saval S.A. Ethanol, HCl, NaOH, and acetone were purchased from Merck S.A. All reagents were of analytical grade. Deionized water was used to prepare the samples.

Equipment

The size and zeta potential of the $NE_{O/W}$ have been measured with a zetasizer Nano-ZS (Malvern Instruments, Worcestershire, UK). For $NE_{O/W}$ preparation, a magnetic stirrer (JEIO TECH, HP 3000) was used. The pH was measured with a pH meter Scholar 425 Corning. Organic solvents were removed by the aid of a rotaryevaporator IKA RV 10 Basic V. The unit used for DF studies consisted of a filtration cell (Amicon 8010, 10 mL capacity) with a magnetic stirrer (Heidolph MR1000), a regenerated cellulose membrane with a molecular-weight cutoff of 5000 Da (Ultracel PLCC; 25 mm diameter), a reservoir (Amicon), a selector (Amicon), and an extra pure (99.995%) N_2 pressure source (AGA). UV–vis analyses were carried out in a Heλios γ spectrophotometer (Thermo Scientific).

Procedures

OTC Stock Solution

A solution of 1.0×10^{-3} M was prepared by dissolving 0.0124 g (2.5×10^{-5} mol) of OTC in 25 mL of ethanol. If needed, the solution was stored in an amber container and refrigerated at 4°C. Alternatively, a stock solution of 1.0×10^{-3} M was prepared by dissolving 0.0124 g (2.5×10^{-5} mol) of OTC in 25 mL of deionized water at pH 2.0. Calibration curves at OTC concentrations ranging between 1.0×10^{-5} and 1.0×10^{-4} M were carried out by UV–vis spectroscopy in water at pH 2.8, 5.0, and 8.0, obtaining molar extinction coefficients of 13,616, 12,656, and 11,765 M^{-1} cm^{-1}, respectively.

Preparation of Ionic $NE_{O/W}$

Ionic $NE_{O/W}$ was prepared by the solvent displacement technique. EPIK (30 mg) was dissolved in 1 mL of ethanol. To this preparation, 125 μL of the mineral oil MIGLYOL 812 was added. In order to control the surface charge of the nanodroplets in the $NE_{O/W}$, different cationic and anionic cosurfactants were added. The cationic BKC (7 mg) or CTAB (8 mg) were dissolved in 9 mL of acetone. The anionic surfactant SDS (7 mg) was dissolved in 20 mL of water. EPIK and all cosurfactant final concentration achieved values around one order of magnitude below their critical micelle concentration. Subsequently the EPIK/ethanol/miglyol solution was mixed with the acetone solution containing a cationic cosurfactant. The resulting organic phase was added to an aqueous phase of 20 mL of deionized water. The formation of $NE_{O/W}$ was instantaneous, resulting in a milky mixture, as can be seen Figure 3. Then, the mixture was rotaevaporated at 40°C to extract the solvents and to concentrate the mixture to a final volume of 10 mL. Anionic $NE_{O/W}$ was prepared by pouring the EPIK/ethanol/miglyol solution into the 20 mL of aqueous phase containing SDS. The addition the OTC to the systems was carried out by adding 1 mL of 1.0×10^{-3} M OTC stock solution in ethanol to the organic phase. The final concentration of OTC in 10 mL of the $NE_{O/W}$ is 1.0×10^{-4} M. The pH of all $NE_{O/W}$ was adjusted with minimum amounts of HCl or NaOH.

Physicochemical Characterization of the $NE_{O/W}$

The size, polydispersity index (PI), and zeta potential of the $NE_{O/W}$ were determined by photon correlation spectroscopy and laser Doppler anemometry, in the zetasizer. The particle size data is reported as the mean diameter. Results were considered valid under the Zetasizer Software 6.20, Malvern. All measurements for each formulation were performed in triplicate, and the corresponding mean value and SD were registered. The stability of the $NE_{O/W}$ was studied by analyzing their size and zeta potential during 60 days at 4°C, 20°C, and 50°C. In addition, the stability of the formulations has been checked after DF by the same methods.

OTC/$NE_{O/W}$ Interaction

The DF technique was used to analyze the OTC interaction with the $NE_{O/W}$ (see Fig. 1).[31,48,50,62,63] $NE_{O/W}$ (10 mL) containing 1.0×10^{-4} M of OTC obtained after rotaevaporation was diafiltered using a regenerated cellulose membrane of molecular-weight cutoff of 5000 Da. The pH of both the aqueous solutions contained in the reservoir and in the cell was adjusted to 2.8, 5.0, and 8.0, depending on the experiment. A total pressure of

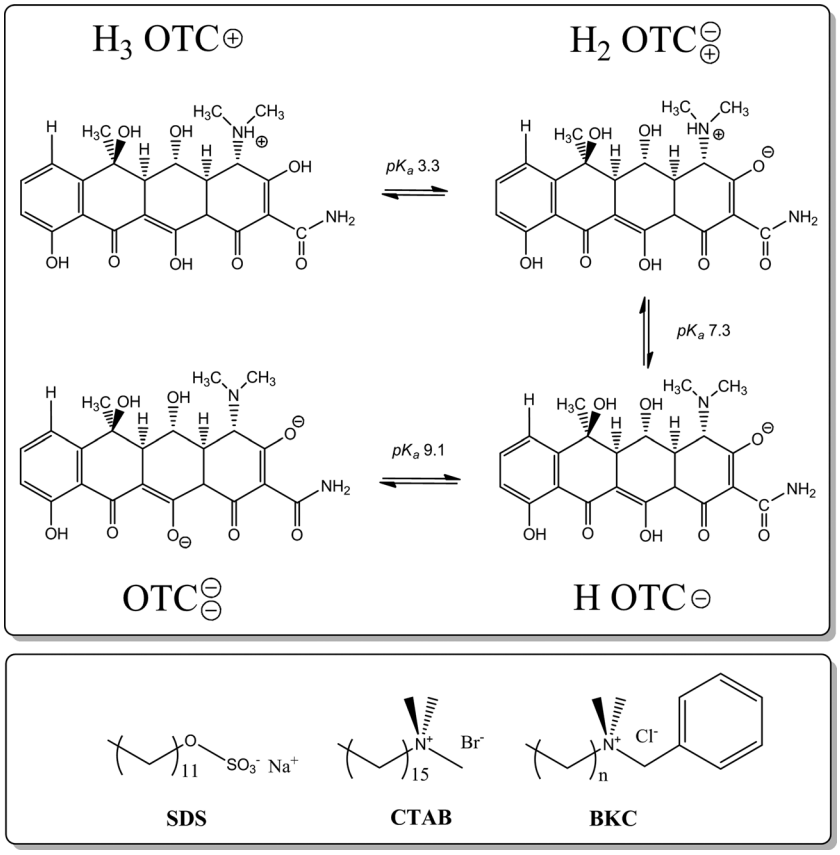

Figure 2. OTC acid–base equilibrium showing cationic behavior under pH 3.3, zwitterionic behavior between pH 3.3 and 7.3, anionic behavior between pH 7.3 and 9.1, and dianionic behavior over pH 9.1; and molecular structures of the anionic and cationic cosurfactants.

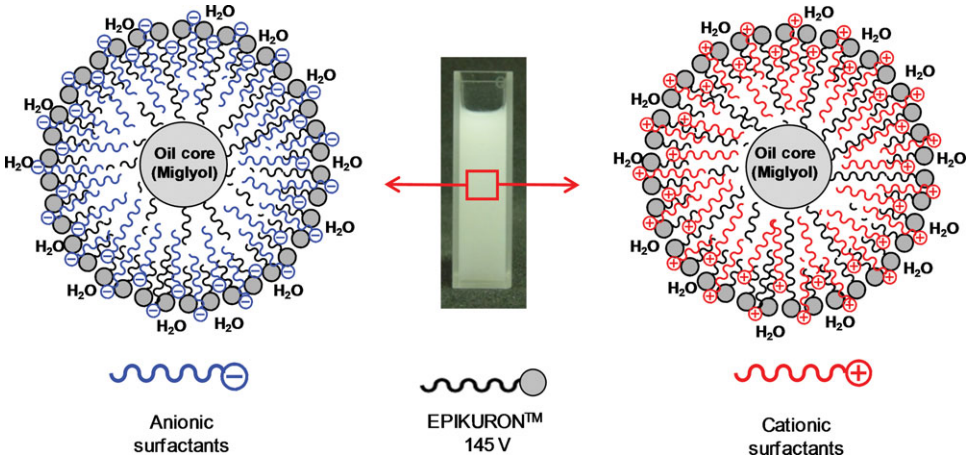

Figure 3. Schematic representation of an anionic (left) and cationic (right) $NE_{O/W}$, and picture of a $NE_{O/W}$ (center) revealing its milky aspect.

3 bar was used for filtration, keeping constant the solution volume in the cell by creating a continuous flux of liquid through the cell solution from the reservoir (between 0.002 and 0.007 mL s^{-1}). Vigorous stirring was held in order to minimize concentration polarization and fouling. Filtration fractions (ranging between 6.0 and 8.0 mL) were collected in test tubes of 10 mL and the OTC concentration in each single fraction was analyzed by UV–vis spectroscopy. Worthy of mention is the large number of conjugated double bonds in OTC (see Fig. 2), allowing its direct quantification using UV–vis spectroscopy. Blank experiments were performed with the same procedure, by diafiltering a pristine 1.0×10^{-4} M of OTC solution. The logarithm of the concentration of OTC in the filtration fractions was then plotted versus F, and the data were adjusted by the linear least-squares method. The slopes of the linear curves were extracted (k^{m} and j), and with the aid of the ordinate at the origin ($< c_{OTC}^{fitrate-init} >$) the values of v, v^{m}, u, and u^{m} are calculated according to Eqs. (21) and (13).

 DOI 10.1002/jps.24255

RESULTS AND DISCUSSION

OTC Physicochemical Properties

Oxytetracycline is a hydrophilic molecule with a solubility of 50 mg/mL in aqueous 1 M HCl. The acid–base characteristics and p*K*a of OTC are known. Three p*K*a are described at values of 3.3 (pK_{a1}), 7.3 (pK_{a2}), and 9.1 (pK_{a3}). An outline of the acid–base equilibrium of this antibiotic is shown in Figure 2. Stephens et al.[64] assigned pK_{a1} to the acid–base characteristics of the hydroxyl vicinal to the dimethyl amino group, so that delocalization of the charge on a trycarbonyl structure is held; pK_{a2} was assigned to the acid–base equilibrium at the dimethylamine group; finally pK_{a3} was assigned to the acid–base equilibrium at the β-diketone group at the center of the molecule, producing stabilization by resonance. This means that the OTC has a cationic behavior at pH lower than 3.3, zwitterionic behavior between pH 3.3 and 7.3, anionic behavior between pH 7.3 and 9.1, and dianionic behavior over pH 9.1. Because of the presence of charges on the molecule, OTC has high solubility in polar solvents whose dielectric constant is comparatively large, such as water, dimethylsulfoxide, acetonitrile, methanol, ethanol, and acetone.[65] In contrast, it shows poor solubility in solvents such as dichloromethane, ethylacetate, or chloroform. Besides, its extended conjugate systems and its heteroatoms may allow undergoing hydrophobic interactions, aromatic–aromatic interactions, and hydrogen bonding.[66,67]

Preparation of Cationic and Anionic $NE_{O/W}$

The formation of $NE_{O/W}$ by solvent displacement is widely described in the literature and is mainly focused in the incorporation of lipophilic molecules into the nanoemulsions.[68–70] These formulations are easily prepared by mixing two phases (organic and aqueous), provided that the organic solvents used are soluble in water, followed by the evaporation of the organic solvents. Reproducible and highly stable formulations using this methodology have been described.[71] Cationic and anionic $NE_{O/W}$ were prepared using different ionic surfactants and adjusting the pH of the medium to values for which OTC is negative, zwiterionic, or positively charged at pH 8.0, 5.0, and 2.8, respectively, thus allowing identifying the influence of the respective charges on the drug/$NE_{O/W}$ interactions. A schematic representation of the nanodroplets is shown in Figure 3.

Table 1 shows size, PI, and zeta potential values of the different $NE_{O/W}$, loaded or not with OTC, at different pH. As said before, $NE_{O/W}$ are complex systems referred to as *systems approaching thermodynamic stability*, whose stability is mainly related to their slow molecular rearrangement kinetics. In this sense, small variations during the $NE_{O/W}$ formation process produce variations on the values of size and zeta potential, so that interpretation of the data should be performed on the basis of rough tendencies concerning size and sign of the zeta potential. All formulations showed submicron sizes in the range of 130–250 nm, each formulation showing nanodroplets of very homogeneous size distribution as denoted by the low PI values found (0.11–0.23). These data are consistent with those previously described in the literature.[1,2,35,72–74] Zeta potentials whose absolute values are higher than 30 mV are considered related to stable systems.[9] EPIK is a mixture of surfactants that include zwitterionic phospholipids, anionic fatty acids, and phosphatidic acid, among others, so that $NE_{O/W}$ containing only EPIK show negative zeta potential. As expected, the addition of BKC or CTAB to the $NE_{O/W}$ formulations at the three pH values produces electrical charge inversion.[35,36] The absolute value of the zeta potential is high enough to guarantee stability of the $NE_{O/W}$ at pH 8.0 and 5.0. However, at pH 2.8, it decreases achieving a value of −19 mV; the incorporation of SDS to the $NE_{O/W}$ allows obtaining a high negative zeta potential (−85 mV), whereas the incorporation of CTAB induces a high positive zeta potential (+51 mV) at this pH. An interesting feature is represented by the formulation containing EPIK loaded with OTC and evaluated at pH 2.8, where visible phase separation occurs. As said before, the $NE_{O/W}$ containing only EPIK shows low negative zeta potential, producing instability that is increased by the incorporation of the antibiotic that at this pH is cationic. This hypothesis is supported by the fact that the addition of SDS to the $NE_{O/W}$ at this pH allows obtaining a stable $NE_{O/W}$ in the presence of OTC, whose zeta potential achieves a value of −74 mV. Molar excess of surfactants over the antibiotic (around 100-fold) makes the antibiotic contribution to neutralization almost negligible.

Table 1. Size, PI, and Zeta Potential of $NE_{O/W}$ in the Absence and the Presence of 1.0×10^{-4} M of OTC at Different pH

Formulation[a]	pH	Size (nm)	PI	Zeta Potential (mV)
EPIK	8.0	136 ± 1.3	0.15	−39 ± 0.7
EPIK–OTC	8.0	160 ± 1.4	0.15	−55 ± 1.1
EPIK–BKC	8.0	252 ± 0.3	0.21	38 ± 0.8
EPIK–BKC–OTC	8.0	227 ± 0.07	0.11	50 ± 1.0
EPIK–CTAB	8.0	237 ± 0.9	0.18	43 ± 0.7
EPIK–CTAB–OTC	8.0	217 ± 0.8	0.23	40 ± 0.1
EPIK	5.0	162 ± 1.3	0.17	−60 ± 1.7
EPIK–OTC	5.0	175 ± 0.2	0.18	−62 ± 2.2
EPIK–BKC	5.0	232 ± 1.0	0.17	57 ± 0.8
EPIK–BKC–OTC	5.0	230 ± 1.1	0.21	53 ± 0.2
EPIK–CTAB	5.0	209 ± 1.5	0.16	71 ± 0.2
EPIK–CTAB–OTC	5.0	218 ± 0.3	0.21	60 ± 1.5
EPIK–SDS	5.0	150 ± 0.1	0.11	−61 ± 0.7
EPIK–SDS–OTC	5.0	152 ± 0.7	0.12	−90 ± 0.7
EPIK	2.8	157 ± 2.0	0.13	−19 ± 2.2
EPIK–OTC	2.8	pp[b]	–	–
EPIK–CTAB	2.8	200 ± 2.0	0.19	51 ± 3.5
EPIK–CTAB–OTC	2.8	210 ± 1.2	0.16	52 ± 1.0
EPIK–SDS	2.8	168 ± 0.4	0.12	−85 ± 1.5
EPIK–SDS–OTC	2.8	170 ± 0.9	0.14	−74 ± 0.8

[a] Each formulation was measured in triplicate.
[b] pp, precipitation.

$NE_{O/W}$/OTC Interaction

Diafiltration is presented in this work as a versatile method to calculate important features regarding OTC association efficiencies to $NE_{O/W}$, namely the distribution of drugs thermodynamically and kinetically bound to the nanosystem by calculation of TB_f and KB_f. The hydrophilic regenerated cellulose membrane was found to be suitable for DF of the $NE_{O/W}$. The pore size of the membrane was chosen to be 5000 Da so that only the passage of free OTC is allowed. DF of the $NE_{O/W}$ in the absence of OTC at pH 2.8, 5.0, and 8.0 showed that, at the end of the process, the corresponding size and zeta potential values are conserved with maximum variations in the order of 10% comparing the values before and after diafiltering. The high affinity of the surfactants to the oil droplets may be responsible for that the presence of free surfactants in the filtrate during

Table 2. Experimental DF Values and Calculated TB_f, KB_f, and AE; $y = \ln(c_{OTC}{}^{filtrate})$; $x = F$; R^2 = Linear Regression Factor

Formulation	pH	v	u	j	u^m	k^m	$K_{OTC}{}^{DIS\text{-}NE}$	Linear Adjustments for the Experimental Data	R^2	TB_f (%)	KB_f (%)	AE (%)
OTC	8				0	0.63		$y = -0.63x - 9.3$	0.99			
EPIK–OTC	8	1.0	0.0	0.63			$\rightarrow .\infty$	$y = -0.63x - 9.5$	0.93	$\rightarrow 0$	$\rightarrow 0$	$\rightarrow 0$
EPIK–BKC–OTC	8	0.9	0.1	0.23			0.36	$y = -0.23x - 10.9$	0.89	57	10	67
EPIK–CTAB–OTC	8	0.7	0.3	0.21			0.32	$y = -0.21x - 11.1$	0.93	47	30	77
OTC	5				0	0.93		$y = -0.93x - 8.9$	0.99			
EPIK–OTC	5	0.86	0.14	0.79			5.25	$y = -0.79x - 9.5$	0.82	13	14	26
EPIK–BKC–OTC	5	1	0	0.56			1.41	$y = -0.56x - 9.8$	0.98	40	0	40
EPIK–CTAB–OTC	5	1	0	0.4			0.70	$y = -0.40x - 10.1$	0.97	57	0	57
EPIK–SDS–OTC	5	0.72	0.28	0.74			3.62	$y = -0.74x - 9.8$	0.99	15	28	43
OTC	2.8				0	0.90		$y = -0.90x - 9.2$	0.99			
EPIK–CTAB–OTC	2.8	1	0	0.8			7.2	$y = -0.80x - 9.3$	0.9	11	0	11
EPIK–SDS–OTC	2.8	0.6	0.4	0.28			0.40	$y = -0.28x - 10.8$	0.85	41	40	81

OTC initial concentration was 1.0×10^{-4} M.

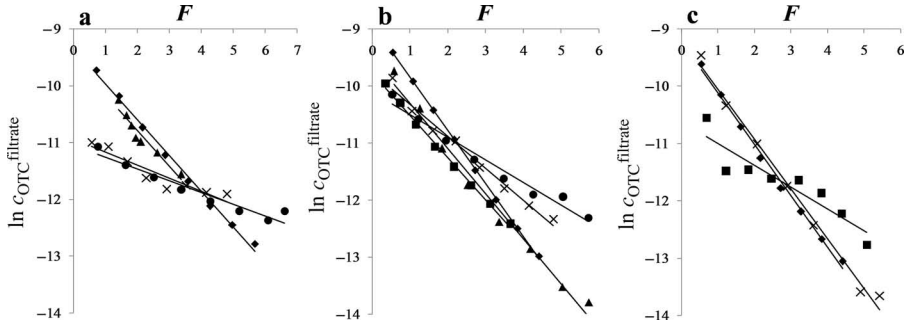

Figure 4. DF profiles at pH 8.0 (a), 5.0 (b), and 2.8 (c) of the formulations containing 1×10^{-4} M of OTC and synthesized according to the experimental section: OTC (♦), EPIK–OTC (▲), EPIK–BKC–OTC (●), EPIK–CTAB–OTC (×), EPIK–SDS–OTC (■).

the DF experiments was found negligible. Similar results are obtained when diafiltering the $NE_{O/W}$ in the presence of the drug, as the $NE_{O/W}$ conserved their integrity, without showing phase separation after 4 h of experiment in which they are subjected to a pressure of 3 bar; the size and zeta potential of the nanosystems studied were also conserved showing maximum variations in the order of 10%.

Blank experiments in which OTC is diafiltered in the absence of the $NE_{O/W}$ show that, according to the literature,[31,33,47,48] the drug does not interact with the DF system at pH 2.8 or 5.0, as the value of k^m reaches 0.9 and 0.93, respectively, as can be seen in Table 2. As expected, a good linear behavior is obtained for the corresponding DF profiles, as can be seen in Figure 4. Low interaction with the DF cell components produces k^m values that tend to 1. On the contrary, OTC interacts with the cell components at pH 8.0, where it is anionic because the corresponding k^m takes a value of 0.63. Besides, the u^m values are 0 at every condition studied, indicating that no antibiotic is irreversibly bound to the DF system. The high pH may induce negative charges on the DF membrane that may produce a slowdown on the rate of elution of the negatively charged antibiotic.

In the presence of the $NE_{O/W}$ contrasting results are obtained. The DF profiles showed in general good linear correlations, as can be seen in Table 2, indicating that the DF analysis can be performed according to the theory developed. The linear adjustments of the data allowed the calculation of the parameters u, v, and j. The most significant values found for the fraction of OTC irreversibly bound to the system, including the $NE_{O/W}$, correspond to the formulations EPIK–BKC–OTC and EPIK–CTAB–OTC at pH 8.0, EPIK–OTC and EPIK–SDS–OTC at pH 5.0, and EPIK–SDS–OTC at pH 2.8, where it took values of 0.1, 0.3, 0.14, 0.28, and 0.4, respectively, as can be deduced by the observation of the u values. The corresponding KB_f values shown in Table 2 can be calculated from Eq. (23). There is a correlation between the charge of the antibiotic, which depends on the pH, and the surface charge of the stabilized nanodroplets. Thus, OTC remains irreversibly retained in the time scale of the DF experiments (3–6 h) at pH 8.0, where is negatively charged, in the presence of the cationic nanoemulsions containing BKC and CTAB, showing KB_f values of 10% and 30%, respectively. It also remains irreversibly bound to the negatively charged $NE_{O/W}$ containing SDS at pH 2.8, at which the antibiotic is positively charged, and a KB_f value of 40% has been found. At pH 5.0, the antibiotic has a zwitterionic nature. However, it tends to be irreversibly retained only in the case of both EPIK–OTC and EPIK–SDS–OTC anionic $NE_{O/W}$. The corresponding KB_f values were found to be 14% and 28%.

Significant interaction values, following the same tendency as in the analysis of the u values, are found analyzing the j values, corresponding to the relative rate of filtration of the antibiotic and related to strength of the interaction of the OTC fraction thermodynamically bound to the system including the $NE_{O/W}$. The j values are extracted from the slope of the DF profiles, and the OTC TB_f values shown in Table 2 can be calculated using Eq. (22). Thus, there is also a correlation between the charge of the antibiotic and the surface charge of the nanodroplets, when checking the j values (see Fig. 4 and Table 2).

At pH 8.0, where the OTC is anionic, low j values as 0.23 and 0.21 are found for both the cationic $NE_{O/W}$ containing BKC and CTAB, respectively, and the respective TB_f values raised to 57% and 47%, respectively. On the contrary, in the absence of the cationic cosurfactants, where the $NE_{O/W}$ showed negative zeta potential, the j value took the same value as k^m indicating negligible reversible interaction between the drug and the nanosystem. At pH 2.8, the same correlation can be found because OTC is cationic, and the respective j values are small when interacting with the negatively charged $NE_{O/W}$ containing SDS, achieving TB_f values of 41%. On the contrary, when CTAB is present in the $NE_{O/W}$ high values of j are found approaching to the corresponding k^m. At pH 5.0, where the OTC is zwitterionic, intermediate values of j are found in the presence of both cationic and anionic $NE_{O/W}$, as expected. However, lower j values have been found for the cationic $NE_{O/W}$ related with higher TB_f values (40% and 57% for the $NE_{O/W}$ containing BKC and CTAB, respectively). The interplay of k^m and j gives rise to $K_{OTC}^{DIS\text{-}NE}$, according to Eq. (15), and the corresponding values related to the discussed TB_f values, are shown in Table 2.

Putting KB_f values and TB_f values together the total AE can be calculated by means of Eqs. (1) and (24). AE achieves values around 80% for OTC at pH 8.0 in the presence of the cationic $NE_{O/W}$ containing BKC or CTAB as well as at pH 2.8 in the presence of the anionic $NE_{O/W}$ containing SDS. At pH 5.0, the values of AE reached 26%–57%, being higher for the cationic $NE_{O/W}$. The overall interaction has a high electrostatic nature because correlations between the *AE* values and the complementarity of the $NE_{O/W}$ charge with respect to that of the antibiotic are found. When charge complementarity is not provided, OTC remains mostly as free molecules in water, indicating that in the $NE_{O/W}$ formation process they are released from the organic phase.

As an important feature of our analysis, we find that the binding mechanisms produce both reversible binding, thus thermodynamically controlled, and irreversible binding, thus kinetically controlled, under our experimental conditions. The thermodynamically controlled binding is related to long-range electrostatic interactions, as seen by the relationship between the distribution constants and the charge complementarity at each pH. Upon long-range electrostatic interactions, the hydrophilic OTC does not lose its hydration sphere and the drug can be considered territorially bound near the surface of the nanodroplets, beyond or at the electric double layer, without producing site-specific binding.[19,22–24] However, because of the high excess of surfactants and corresponding counterions (around 100-fold over the antibiotic), other interactions, such as hydrophobic interactions, must be present that justifies that the OTC–$NE_{O/W}$ interaction is not completely screened. The irreversibility of the binding may be related to the presence of OTC molecules confined in the electric double layer around the nanodroplet. In addition, as seen in other systems,[24,26,28,33] the structure of the antibiotic, presenting extensive conjugate systems and high planarity, may induce short-range site-specific interactions such as hydrogen bonds, aromatic–aromatic interactions, and/or short-range electrostatic interactions that may increase the retention of the drug by the nanoemulsion. Upon formation of ion pairs, the OTC hydration sphere may be partially or totally lost, and the drug can locate in the less superficial area of the nanodroplet interface, or even in the core, as the ion pairs may be stabilized in a hydrophobic environment. To the formation of these ion pairs, short-range electrostatic interactions, hydrophobic, and aromatic–aromatic interactions may contribute. It is interesting to note that the different cosurfactants induce a different ratio between reversible and irreversible binding. Thus, at pH 8.0, CTAB produces an increase on the KB_f value (thus an increase on the irreversibility of the binding) and a decrease on the TB_f value (thus a decrease on the reversibility of the binding) with respect to BKC. At pH 5, the anionic $NE_{O/W}$ enhances an irreversible binding mechanism, whilst the cationic $NE_{O/W}$ containing BKC or CTAB produce only reversible binding. Related to this, the high AE found should be regarded not only as the confinement of OTC in the nanodroplets, but also as the partition of antibiotic molecules between bulk water and the nanodroplet surface, undergoing fast chemical exchange.

Stability of the $NE_{O/W}$

Stability is a critical issue in the development of nanocarrier formulations. Variations on temperature are known to significantly compromise the stability of colloidal systems in time, and show evident importance during storage.[75] The increase on the size of the formulations could be attributed to the weakening and breaking-down of interactions between the molecules that form the nanocarriers, and may alter their drug release and induce destabilization of the formulations. A decrease on size could also occur due to the detachment of components from the nanocarriers or to an increase on the interaction strengths between linkers, potentially affecting the desired efficacy of the nanocarrier.[35] In the present study we evaluated, for a period of 60 days, the stability under conditions that represents refrigeration (4°C), room temperature (25°C), and extreme temperatures (50°C) of anionic and cationic $NE_{O/W}$ loaded with OTC showing high AE at pH 2.8, 5.0, and 8.0 without been subjected to DF. The results can be seen in Figure 5. The formulations at 4°C and 25°C were stable during the storage irrespective of the pH conditions up to 60 days, and the PI remained between 0.11

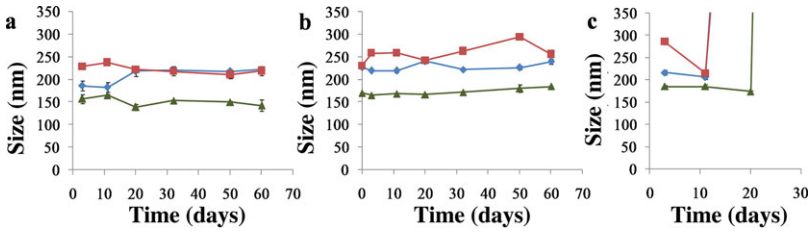

Figure 5. Size (mean ± SD; $n = 3$) of $NE_{O/W}$ containing 1×10^{-4} M of OTC as a function of time, at 4°C (a), 25°C (b), and 50°C (c). Cationic $NE_{O/W}$ containing BKC were evaluated at pH 8.0 (◆) and 5.0 (■). Anionic $NE_{O/W}$ containing SDS was evaluated at pH 2.8 (▲).

and 0.25. The overall trend of prolonged stability is justified by the electrostatic repulsive effect due to the high zeta potential values of the nanosystems. However, formulations subjected to thermal stress of 50°C were stable only for 10 days at pH 5.0 and 8.0, and 20 days at pH 2.8. These results would indicate that our formulations could be protected from acute thermal shock without losing their integrity. In the absence of the OTC, the corresponding nanoemulsions showed comparable stability profiles, being less stable at 50°C.

Final Remarks

Ionic $NE_{O/W}$ represents very interesting means of controlling the release of a variety of lipophilic drugs, but the incorporation of hydrophilic drugs may be difficult due to their high affinity towards water. However, ionic $NE_{O/W}$ may undergo electrostatic interactions, together with hydrophobic, hydrogen bonding, or aromatic–aromatic interactions, with ionic drugs that may enhance the binding of the drug to the stabilized nanodroplets. Considering that more than 75% of the drugs available in the market show weak acid/base properties and aromatic functional groups, the study of their interaction with ionic vehicles is strategic to achieve new formulations that improve bioavailability, prolong the effect in selected tissues, and provide long stability against enzymatic degradation.[60] The interaction between hydrophilic drugs and the nanovehicles may produce irreversible binding, so that the drug release is kinetically controlled by diffusion or erosion, or reversible binding, so that the drug undergoes fast exchange between the nanovehicle and the bulk. Differentiating these two types of mechanisms is important to characterize new formulations for oral, topic, or systemic administration of ionizable drugs.

The potential of the DF technique to determine the AE of ionic drugs to nanovehicles and differentiate the fraction of molecules reversibly and irreversibly bound has been highlighted in this study. The technique is supported by a mathematical development that furnish, after data treatment, the above mentioned important information that may be pivotal during galenic development of controlled release formulations. The results obtained with the antibiotic OTC showed a dependence of the fraction of drug reversible and irreversible bound to the ionic $NE_{O/W}$ on the type of surfactants used to form the nanovehicles. These results not only open new perspectives of formulation to tetracyclines, but also to a variety of important therapeutic ionizable drugs. Ionic $NE_{O/W}$ synthesis can be easily implemented in pharmaceutical and cosmetic industries, requiring similar procedures and machinery to produce conventional formulations.[76] The new analytical possibilities for pharmaceutical technology that DF opens may be used not only at an academic level, but also in the pharmaceutical industry as routine assays to achieve better characterizations and implement quality control procedures.

CONCLUSIONS

Cationic and anionic nanoemulsions containing the antibiotic OTC were obtained at three different pH (2.8, 5.0, and 8.0), displaying sizes between 150 and 230 nm, stable for 60 days at 4°C and 25°C. They showed controllable zeta potential, related to the charge of the surfactants used. As a novelty of the present study, we show that the constant volume DF technique allows determining not only association efficiencies of the drug to $NE_{O/W}$, but also the fraction of the antibiotic reversibly bound, whose release is subjected to thermodynamic control, and irreversibly bound, whose release is subjected to kinetic control. It was found that the hydrophilic antibiotic OTC is bound both reversibly and irreversibly to the nanodroplets, and the extent of reversible and irreversible binding depended on the cosurfactant used. Electrostatic forces are held between the drug and the nanodroplets, which should act as charged particles. Formulations furnishing complementary charge between the antibiotic and the nanoemulsion showed OTC association efficiencies of around 80%, showing 11%–57% of reversible binding, and 10%–40% of irreversible binding. These results highlight the potential of DF as a tool to quantitatively evaluate drug association and release in new drug delivery systems that include bioactive molecules for improved therapies, and as routine assays in academia and pharmaceutical industries.

ACKNOWLEDGMENT

The authors thank FONDECYT (grants No. 3110153, 11121481, and 1120514) for financial support.

REFERENCES

1. Calvo P, VilaJato JL, Alonso MJ. 1996. Comparative in vitro evaluation of several colloidal systems, nanoparticles, nanocapsules, and nanoemulsions, as ocular drug carriers. J Pharm Sci 85(5):530–536.
2. Liu CH, Yu SY. 2010. Cationic nanoemulsions as non-viral vectors for plasmid DNA delivery. Colloids Surf B Biointerfaces 79(2):509–515.
3. Fernandez P, André V, Rieger J, Kühnle A. 2004. Nano-emulsion formation by emulsion phase inversion. Colloids Surf A Physicochem Eng Aspects 251(1–3):53–58.
4. Milton J. Rosen E. 1984. Structure/performance relationships in surfactants. New York: American Chemical Society.
5. Peng L-C, Liu C-H, Kwan C-C, Huang K-F. 2010. Optimization of water-in-oil nanoemulsions by mixed surfactants. Colloids Surf A Physicochem Eng Aspects 370(1–3):136–142.
6. Gautam KK, Tyagi VK. 2006. Microbial surfactants: A review. J Oleo Sci 55(4):155–166.
7. Tadros T, Izquierdo P, Esquena J, Solans C. 2004. Formation and stability of nano-emulsions. Adv Colloid Interface Sci 108–109(0):303–318.
8. Fryd MM, Mason TG. 2012. Advanced nanoemulsions. Annu Rev Phys Chem 63:493–518.
9. de Morais JM, dos Santos ODH, Delicato T, da Rocha-Filho PA. 2006. Characterization and evaluation of electrolyte influence on canola oil/water nano-emulsion. J Dispers Sci Technol 27(7):1009–1014.
10. Atkins PWPJd. 2002. Atkins' physical chemistry. New York: Oxford University Press.
11. Attard P. 2001. Recent advances in the electric double layer in colloid science. Curr Opin Colloid Interface Sci 6(4):366–371.
12. Ahmed K, Li Y, McClements DJ, Xiao H. 2012. Nanoemulsion- and emulsion-based delivery systems for curcumin: Encapsulation and release properties. Food Chem 132(2):799–807.
13. Kabri TH, Arab-Tehrany E, Belhaj N, Linder M. 2011. Physicochemical characterization of nano-emulsions in cosmetic matrix enriched on omega-3. J Nanobiotechnol 9:41.
14. Al-Edresi S, Baie S. 2009. Formulation and stability of whitening VCO-in-water nano-cream. Int J Pharm 373(1–2):174–178.
15. Cano-Salazar LF, Juarez-Ordaz AJ, Gregorio-Jauregui KM, Martinez-Hernandez JL, Rodriguez-Martinez J, Ilyina A. 2011. Ther-

modynamics of chitinase partitioning in soy lecithin liposomes and their storage stability. Appl Biochem Biotechnol 165(7–8):1611–1627.
16. Ahmed M, Ramadan W, Rambhu D, Shakeel F. 2008. Potential of nanoemulsions for intravenous delivery of rifampicin. Pharmazie 63(11):806–811.
17. Donsì F, Sessa M, Mediouni H, Mgaidi A, Ferrari G. 2011. Encapsulation of bioactive compounds in nanoemulsion- based delivery systems. Procedia Food Sci. 1(0):1666–1671.
18. Pool H, Mendoza S, Xiao H, McClements DJ. 2013. Encapsulation and release of hydrophobic bioactive components in nanoemulsion-based delivery systems: Impact of physical form on quercetin bioaccessibility. Food Funct 4(1):162–174.
19. Manning GS. 2007. Counterion condensation on charged spheres, cylinders, and planes†. J Phys Chem B 111(29):8554–8559.
20. Manning GS. 2010. The interaction between a charged wall and its counterions: A condensation theory. J Phys Chem B 114(16):5435–5440.
21. Manning GS. 1969. Limiting laws and counterion condensation in polyelectrolyte solutions I. colligative properties. J Chem Phys 51(3):924–933.
22. Manning GS. 1978. The molecular theory of polyelectrolyte solutions with applications to the electrostatic properties of polynucleotides. Q Rev Biophys 11(02):179–246.
23. Manning GS. 1984. Limiting laws and counterion condensation in polyelectrolyte solutions. 8. Mixtures of counterions, species selectivity, and valence selectivity. J Phys Chem 88(26):6654–6661.
24. Nordmeier E. 1995. Advances in polyelectrolyte research: Counterion binding phenomena, dynamic processes, and the helix-coil transition of DNA. Macromol Chem Phys 196(5):1321–1374.
25. Moreno-Villoslada I, Jofre M, Miranda V, Chandia P, Gonzalez R, Hess S, Rivas BL, Elvira C, San Roman J, Shibue T, Nishide H. 2006. pi-Stacking of rhodamine B onto water-soluble polymers containing aromatic groups. Polymer 47(19):6496–6500.
26. Moreno-Villoslada I, Torres C, González F, Shibue T, Nishide H. 2009. Binding of methylene blue to polyelectrolytes containing sulfonate groups. Macromol Chem Phys 210(13–14):1167–1175.
27. Moreno-Villoslada I, Torres-Gallegos Cs, Araya-Hermosilla R, Nishide H. 2010. Influence of the linear aromatic density on methylene blue aggregation around polyanions containing sulfonate groups. J Phys Chem B 114(12):4151–4158.
28. Moreno-Villoslada I, Gonzalez F, Rivera L, Hess S, Rivas BL, Shibue T, Nishide H. 2007. Aromatic–aromatic interaction between 2,3,5-triphenyl-2H-tetrazolium chloride and poly(sodium 4-styrenesulfonate). J Phys Chem B 111(22):6146–6150.
29. Manning GS. 2011. Counterion condensation theory of attraction between like charges in the absence of multivalent counterions. Eur Phys J E 34(12):1–18.
30. Moreno-Villoslada I, González F, Arias L, Villatoro JM, Ugarte R, Hess S, Nishide H. 2009. Control of C.I. Basic Violet 10 aggregation in aqueous solution by the use of poly(sodium 4-styrenesulfonate). Dyes Pigments 82(3):401–408.
31. Moreno-Villoslada I, Miranda V, Gutiérrez R, Hess S, Muñoz C, Rivas BL. 2004. Interactions of 2,3,5-triphenyl-2H-tetrazolium chloride with poly(sodium 4-styrenesulfonate) studied by diafiltration and UV–vis spectroscopy. J Membr Sci 244(1–2):205–213.
32. Moreno-Villoslada I, Torres C, Gonzalez F, Soto M, Nishide H. 2008. Stacking of 2,3,5-triphenyl-2H-tetrazolium chloride onto polyelectrolytes containing 4-styrenesulfonate groups. J Phys Chem B 112(36):11244–11249.
33. Moreno-Villoslada I, González R, Hess S, Rivas BL, Shibue T, Nishide H. 2006. Complex formation between rhodamine B and poly(sodium 4-styrenesulfonate) studied by ^{1}H-NMR. J Phys Chem B 110(43):21576–21581.
34. Araya-Hermosilla R, Araya-Hermosilla E, Torres-Gallegos C, Alarcón-Alarcón C, Moreno-Villoslada I. 2013. Sensing Cu^{2+} by controlling the aggregation properties of the fluorescent dye rhodamine 6G with the aid of polyelectrolytes bearing different linear aromatic density. React Funct Polym 73(11):1455–1463.
35. Oyarzun-Ampuero FA, Rivera-Rodríguez GR, Alonso MJ, Torres D. 2013. Hyaluronan nanocapsules as a new vehicle for intracellular drug delivery. Eur J Pharm Sci 49(4):483–490.
36. Rivera-Rodríguez GR, Alonso MJ, Torres D. 2013. Poly-L-asparagine nanocapsules as anticancer drug delivery vehicles. Eur J Pharm Biopharm 85(3, Part A):481–487.
37. Rivera-Rodriguez GR, Lollo G, Montier T, Benoit JP, Passirani C, Alonso MJ, Torres D. 2013. In vivo evaluation of poly-L-asparagine nanocapsules as carriers for anti-cancer drug delivery. Int J Pharm 458(1):83–89.
38. Zhao L, Wei Y, Huang Y, He B, Zhou Y, Fu J. 2013. Nanoemulsion improves the oral bioavailability of baicalin in rats: In vitro and in vivo evaluation. Int J Nanomed 8:3769–3779.
39. Sharma S, Sahni JK, Ali J, Baboota S. Effect of high-pressure homogenization on formulation of TPGS loaded nanoemulsion of rutin—Pharmacodynamic and antioxidant studies. Drug Deliv 0(0):1–11.
40. Mason TG, Wilking JN, Meleson K, Chang CB, Graves SM. 2006. Nanoemulsions: Formation, structure, and physical properties. J Phys Condens Matter 18(41):R635.
41. Jiang SP, He SN, Li YL, Feng DL, Lu XY, Du YZ, Yu HY, Hu FQ, Yuan H. 2013. Preparation and characteristics of lipid nanoemulsion formulations loaded with doxorubicin. Int J Nanomed 8:3141–3150.
42. Guo Y, Liu X, Sun X, Zhang Q, Gong T, Zhang Z. 2012. Mannosylated lipid nano-emulsions loaded with lycorine-oleic acid ionic complex for tumor cell-specific delivery. Theranostics 2(11):1104–1114.
43. Hutter E, Boridy S, Labrecque S, Lalancette-Hébert M, Kriz J, Winnik FM, Maysinger D. 2010. Microglial response to gold nanoparticles. ACS Nano 4(5):2595–2606.
44. Liew MWO, Chuan YP, Middelberg APJ. 2012. Reactive diafiltration for assembly and formulation of virus-like particles. Biochem Eng J 68(0):120–128.
45. Kliushnik S, McHedlishvili BV, Gribencha SV, Romanova LN, Barinskii IF. 1991. The purification and concentration of the rabies virus by a diafiltration concentration method. Vopr Virusol 36(5):394–399.
46. Moreno-Villoslada I, Fuenzalida JP, Tripailaf G, Araya-Hermosilla R, Pizarro Gdel C, Marambio OG, Nishide H. 2010. Comparative study of the self-aggregation of rhodamine 6G in the presence of poly(sodium 4-styrenesulfonate), poly(N-phenylmaleimide-co-acrylic acid), poly(styrene-alt-maleic acid), and poly(sodium acrylate). J Phys Chem B 114(37):11983–11992.
47. Moreno-Villoslada I, Jofré M, Miranda V, González R, Sotelo T, Hess S, Rivas BL. 2006. pH dependence of the interaction between rhodamine B and the water-soluble poly(sodium 4-styrenesulfonate). J Phys Chem B 110(24):11809–11812.
48. Moreno-Villoslada I, Miranda V, Jofré M, Chandía P, Villatoro JM, Bulnes JL, Cortés M, Hess S, Rivas BL. 2006. Simultaneous interactions between a low molecular-weight species and two high molecular-weight species studied by diafiltration. J Membr Sci 272(1–2):137–142.
49. Moreno-Villoslada I, Oyarzún F, Miranda V, Hess S, Rivas BL. 2005. Comparison between the binding of chlorpheniramine maleate to poly(sodium 4-styrenesulfonate) and the binding to other polyelectrolytes. Polymer 46(18):7240–7245.
50. Rivas BL, Pereira ED, Moreno-Villoslada I. 2006. Highlights on the use of diafiltration in the characterization of the low molecular-weight species-water soluble polymer interactions. In Frontal polymer research; Bregg RK, Ed. New York: Nova Science Publishers.
51. Wachsmann P, Lamprecht A. Ethylcellulose nanoparticles with bimodal size distribution as precursors for the production of very small nanoparticles. Drug Dev Ind Pharm 0(0):1–7.
52. Fuenzalida JP, Flores ME, Móniz I, Feijoo M, Goycoolea F, Nishide H, Moreno-Villoslada I. 2014. Immobilization of hydrophilic low molecular-weight molecules in nanoparticles of chitosan/poly(sodium 4-styrenesulfonate) assisted by aromatic–aromatic interactions. J Phys Chem B 118(32):9782–9791.

53. Miao F, Velayudhan A, DiBella E, Shervin J, Felo M, Teeters M, Alred P. 2009. Theoretical analysis of excipient concentrations during the final ultrafiltration/diafiltration step of therapeutic antibody. Biotechnol Prog 25(4):964–972.
54. Li Y, Corredig M. 2014. Calcium release from milk concentrated by ultrafiltration and diafiltration. J Dairy Sci. 97(9):5294–5302.
55. Chopra I, Roberts M. 2001. Tetracycline antibiotics: Mode of action, applications, molecular biology, and epidemiology of bacterial resistance. Microbiol Mol Biol Rev 65(2):232–260; second page, table of contents.
56. Marshall BM, Levy SB. 2011. Food animals and antimicrobials: Impacts on human health. Clin Microbiol Rev 24(4):718–733.
57. Yano Y, Hamano K, Satomi M, Tsutsui I, Aue-umneoy D. 2011. Diversity and characterization of oxytetracycline-resistant bacteria associated with non-native species, white-leg shrimp (*Litopenaeus vannamei*), and native species, black tiger shrimp (Penaeus monodon), intensively cultured in Thailand. J Appl Microbiol 110(3):713–722.
58. Dang H, Zhang X, Song L, Chang Y, Yang G. 2007. Molecular determination of oxytetracycline-resistant bacteria and their resistance genes from mariculture environments of China. J Appl Microbiol 103(6):2580–2592.
59. Kümmerer K. 2003. Significance of antibiotics in the environment. J Antimicrob Chemother 52(1):5–7.
60. Marcato PD, Duran N. 2008. New aspects of nanopharmaceutical delivery systems. J Nanosci Nanotechnol 8(5):2216–2229.
61. Zhang L, Pornpattananangku D, Hu CM, Huang CM. 2010. Development of nanoparticles for antimicrobial drug delivery. Curr Med Chem 17(6):585–594.
62. Rivas BL, Pereira ED, Moreno-Villoslada I. 2003. Water-soluble polymer–metal ion interactions. Prog Polym Sci 28(2):173–208.
63. Rivas BL, Schiappacasse LN, Pereirau E, Moreno-Villoslada I. 2004. Error simulation in the determination of the formation constants of polymer-metal complexes (PMC) by the liquid-phase polymer-based retention (LPR) technique. J Chilean Chem Soc 49:345–350.
64. Stephens CR, Murai K, Brunings KJ, Woodward RB. 1956. Acidity constants of the tetracycline antibiotics. J Am Chem Soc 78(16):4155–4158.
65. Toral MI, Orellana S, Soto C, Richter P. 2011. Extraction and determination of oxytetracycline hydrochloride and oxolinic acid in fish feed by derivative spectrophotometry of first order. Food Anal Methods 4(4):497–504.
66. Kumar R, Betageri GV, Gupta RB. 1998. Partitioning of oxytetracycline between aqueous and organic solvents: Effect of hydrogen bonding. Int J Pharm 166(1):37–44.
67. Chi Z, Liu R, Zhang H. 2010. Noncovalent interaction of oxytetracycline with the enzyme trypsin. Biomacromolecules 11(9):2454–2459.
68. Trimaille T, Chaix C, Delair T, Pichot C, Teixeira H, Dubernet C, Couvreur P. 2001. Interfacial deposition of functionalized copolymers onto nanoemulsions produced by the solvent displacement method. Colloid Polym Sci 279(8):784–792.
69. Dixit N, Kohli K, Baboota S. 2008. Nanoemulsion system for the transdermal delivery of a poorly soluble cardiovascular drug. PDA J Pharm Sci Technol 62(1):46–55.
70. Shakeel F, Baboota S, Ahuja A, Ali J, Aqil M, Shafiq S. 2007. Nanoemulsions as vehicles for transdermal delivery of aceclofenac. AAPS Pharmscitech 8(4).
71. Anton N, Benoit JP, Saulnier P. 2008. Design and production of nanoparticles formulated from nano-emulsion templates—A review. J Control Release 128(3):185–199.
72. Lozano MV, Lollo G, Alonso-Nocelo M, Brea J, Vidal A, Torres D, Alonso MJ. 2013. Polyarginine nanocapsules: A new platform for intracellular drug delivery. J Nanopart Res 15(3):1–14.
73. Prego C, García M, Torres D, Alonso MJ. 2005. Transmucosal macromolecular drug delivery. J Control Release 101(1–3):151–162.
74. Oyarzun-Ampuero F, Garcia-Fuentes M, Torres D, Alonso M. 2010. Chitosan-coated lipid nanocarriers for therapeutic applications. J Drug Deliv Sci Technol 20(4):259–265.
75. Freitas C, Müller RH. 1998. Effect of light and temperature on zeta potential and physical stability in solid lipid nanoparticle (SLN^{TM}) dispersions. Int J Pharm 168(2):221–229.
76. Rodriguez-Abreu C, Vila A. 2014. Nano-droplet systems by surfactant self-assembly and applications in the pharmaceutical industry. Curr Top Med Chem 14(6):747–765.